

RSC Advances



This is an *Accepted Manuscript*, which has been through the Royal Society of Chemistry peer review process and has been accepted for publication.

Accepted Manuscripts are published online shortly after acceptance, before technical editing, formatting and proof reading. Using this free service, authors can make their results available to the community, in citable form, before we publish the edited article. This *Accepted Manuscript* will be replaced by the edited, formatted and paginated article as soon as this is available.

You can find more information about *Accepted Manuscripts* in the [Information for Authors](#).

Please note that technical editing may introduce minor changes to the text and/or graphics, which may alter content. The journal's standard [Terms & Conditions](#) and the [Ethical guidelines](#) still apply. In no event shall the Royal Society of Chemistry be held responsible for any errors or omissions in this *Accepted Manuscript* or any consequences arising from the use of any information it contains.

COMMUNICATION

Fabrication and Modification of Composite Silica Nano Test Tubes for Targeted Drug Delivery

Cite this: DOI: 10.1039/x0xx00000x

F. Buyukserin^{a*}, S. Altuntas^b and B. Aslim^c

Received 00th January 2014,

Accepted 00th January 2014

DOI: 00.0000/x0xx00000x

www.rsc.org/

This work describes the use of template synthesis to fabricate multifunctional composite silica nano test tubes for targeted drug delivery. The tubular nanostructures were formed within nanoporous anodized alumina templates and their inner voids were filled with a drug-bearing gel matrix while the test tubes were embedded within the template. Upon template removal, the composite nanocarriers were biofunctionalized with a targeting moiety towards breast cancer cells. The results show that targeting is critical in inducing cell death and the targeted nanocarriers are extensively more cytotoxic towards cancer cells compared with healthy controls.

Introduction

Employing nanoparticles for drug delivery becomes increasingly important as they display improved biological properties involving increased efficacy and reduced systemic toxicity.^{1,2} Directing these nanocarriers through biofunctionalization of the particle surface allows efficient delivery and accumulation of therapeutic agents to target sites in the body.^{3,4} Conventionally, particles with spherical shapes are used as the delivery vehicles, however, recent results about the improved biological properties of non-spherical particles are beginning to question this tendency. For example, increased tumor accumulation⁵ and blood circulation⁶ were reported for 1-Dimensional (1D) nanoparticles compared with spherical counterparts. Successful drug delivery studies with carbon, polymer and silica-based nanotubes^{7,8} also contributed to the increased attention for the utilization of non-spherical nanocarriers.

Silica nanotubes and nano test tubes (SNTs)⁹⁻¹⁵ are novel 1D inorganic structures with several desired characteristic for biomedical applications involving ease of synthesis and modification, large controllable inner voids for drug loading, low toxicity, extensive dispersion etc.¹⁰ They are typically prepared by template synthesis¹⁶ which is a powerful method to create nanorods and nanotubes of different materials within the pores of a template membrane. Nanoporous anodized aluminum oxide (AAO) is generally used as the template material for SNT production.

Multifunctional SNTs can be fabricated by template synthesis through differential modification strategy that encompasses the independent functionalization of the inner vs. the outer surfaces of the nanotubes.^{10,12} Various applications of SNTs involving biosensors,¹¹ biomolecule separation,¹² cell labeling,¹³ cell recognition¹⁰ and drug/gene delivery^{14,15} have been successfully demonstrated. Very recently, Sang Bok Lee and coworkers have reported a stimuli-responsive SNT formulation¹⁷ for the treatment of drug resistant cancer cells. Despite these advances, the use of SNTs for targeted drug delivery has not been demonstrated. Moreover, the drug loading strategy of the related reports has been limited to ionic interactions.

Here we report, for the first time, targeted drug delivery with multifunctional composite SNTs. A unique template-based approach that employs the whole interior volume of SNTs for drug-bearing gel loading has been utilized. Upon targeting with folate groups, multifunctional agents were created which showed extensive cytotoxicity towards cancer cells compared with healthy ones. A prominent feature of SNTs is the greater extent of cell death with lesser effective drug concentrations. The details of SNT fabrication, modification and characterization as well as the viability studies with cancer and normal cells are described.

Experimental

Materials

Aluminum foil (99.998%), N-Hydroxysuccinimide (NHS) and 2,2-diethoxyacetophenone were obtained from Alfa Aesar. Hydroxyethylmethacrylate (HEMA), poly(ethylene glycol)

^a Department of Biomedical Engineering, TOBB Univ. of Economics & Technology, Ankara 06560, TR.

^b Micro and Nanotechnology Graduate Program, TOBB Univ. of Economics & Technology, Ankara 06560, TR.

^c Department of Biotechnology, Faculty of Science, Gazi University, Ankara 06500, TR.

*Corresponding author, E-mail: fbuyukserin@etu.edu.tr

ethylether methacrylate (PEG-EEM), 2-aminoethylmethacrylate hydrochloride (AEM), trimethylolpropane ethoxylate triacrylate, fluorescein-o-acrylate, doxorubicin (DOX) hydrochloride, 3-Aminopropyltriethoxy silane (APTES), 1-Ethyl-3-(3-dimethylaminopropyl)carbodiimide (EDC) and n-hexane were used as received from Sigma-Aldrich, as were Oxalic acid from Acros Organics, H_3PO_4 from BDH Prolabo, CrO_3 and H_2SO_4 from Fluka. SiCl_4 , folic acid (FA), ethanol (EtOH) and 2-propanol (IPA) were obtained from Merck. A Sartorius water purification system was used to obtain purified water. The consumables related with the cell studies were obtained from invitrogen.

Preparation of AAO Membrane, SNTs and Composite SNTs

A two-step anodization method¹⁸ was followed to prepare AAO templates with ordered nanopores in oxalic acid electrolyte. The cylindrical nanopores of the AAO membrane were then used as templates to fabricate SNTs via surface sol-gel method¹⁹ which entails layer-by-layer deposition of silica onto a substrate material. The details of the two-step anodization and surface sol-gel methods were described in the Supplementary Information section. In order to obtain free SNTs, the top surface silica layer which normally connects the tubular structures had to be removed.²⁰ This was conducted by a brief Ar^+ plasma treatment (1 min) using a SAMCO RIE-1C reactive ion etcher system. When necessary, naked SNTs were obtained after this stage by removing the template in 0.1 M NaOH.

Composite SNTs were prepared by placing the silica deposited AAO template in a prepolymer solution containing HEMA, PEG-EEM, AEM, trimethylolpropane ethoxylate triacrylate, doxorubicin (DOX) hydrochloride, 2,2-diethoxyacetophenone, IPA and water (see Table S1 in the Supplementary information for relative ratios). It should be noted that, as a co-monomer, fluorescein-o-acrylate was also used in some cases for characterization purposes. The template was kept in this solution for 3 h and sonicated occasionally to prevent bubble formation within the nanopores. After the incubation period, the template was exposed to UV-radiation for 10 min (UVP Brand, 365 nm, 12 mW/cm²). This caused gel formation within the nanopores of silica deposited template as well as its top surface. The surface gel was removed by a doctor blade and the template was immersed in 20 % H_3PO_4 solution in order to dissolve AAO and liberate free composite SNTs.

Modification and Characterization of SNTs and Composite SNTs

SNTs and composite SNTs without any outer surface modification were characterized by TEM. After the template removal, the tubular nanostructures were collected by a filtration membrane, rinsed extensively with purified water and EtOH, and then dispersed in EtOH. TEM images were obtained from a FEI Tecnai G² Spirit TEM microscope after a tiny volume (100 μl) of this dispersion was dropped on a copper grid. Fluorescence microscopy was also utilized for the characterization of composite SNTs. For fluorescence images, longer composite SNTs were prepared from ~ 4 μm -deep AAO templates. Here, the gel matrix involved an additional fluorescein-o-acrylate component (0.075 % wt/vol) instead of DOX for improved image quality. The resultant composite SNTs were filtered and placed on a glass slide and then imaged by using an Olympus Fluorescence Microscope with an excitation wavelength between 480-500 nm. The same composite SNT sample was also characterized by TEM in order to confirm uniform gel filling along the tube length.

The FA modification and characterization studies were conducted by using naked SNTs for simplicity reasons. In order to obtain FA coupling, an amine modification²¹ was first conducted on the outer surfaces of SNTs and these amine groups were then reacted with EDC activated FA solution. The FA modification of SNTs were characterized by zeta potential, FTIR and XPS studies. See Supplementary Information for experimental conditions regarding FA coupling as well as preparation of samples for characterization.

Cells and Culture

SK-BR3 breast cancer cells (ATCC) and MCF-12A normal human mammary gland epithelial cells (ATCC) were used in the cell studies and the cell viabilities were examined via WST-1 Cell Proliferation Kit Assay (See Supplementary Information for the experimental details of cell culture and viability studies). The SNT concentrations in the cell viability studies were reported by using a predetermined AAO template area and a calculated pore density of ~ 7.10⁹ pores/cm². Here, Image J software was used on SEM images of AAO membranes to obtain the pore density value.

Results and Discussion

The scheme for the fabrication of composite SNTs is illustrated in Fig. 1. An AAO membrane with ordered nanopores was produced by two-step anodization protocol¹⁸ and used as a template to prepare the nanostructures. This template was first deposited with a nanoscale silica coating via surface sol-gel method¹⁹ and the top surface silica coating that normally connects individual particles was removed by Ar^+ plasma treatment.¹⁰ The silica-coated template was then immersed in a prepolymer solution that contains DOX in addition to a group of different monomers (Table S1). After 10 min UV-based crosslinking period, the top gel layer formed on the AAO template surface was removed by a doctor blade and the gel-filled composite SNTs were liberated by template dissolution in H_3PO_4 solution.

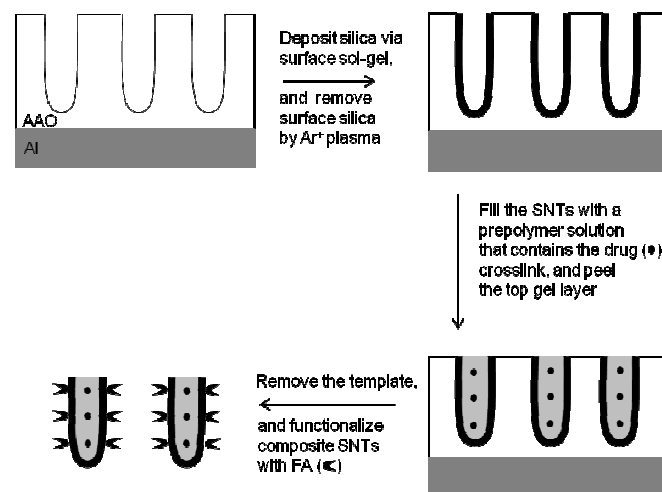


Fig. 1. The schematic for the preparation of biofunctionalized composite SNTs.

Fig. 2A shows surface SEM image of the AAO template prepared via two-step anodization method. The template was deposited with silica to obtain SNTs that can be liberated by dissolving the amphoteric template. (Fig. 2B). The dimensions of the SNTs can be tuned by controlling the template depth and pore diameter. In this study SNTs with 123 ± 14 nm diameter and 820 ± 99

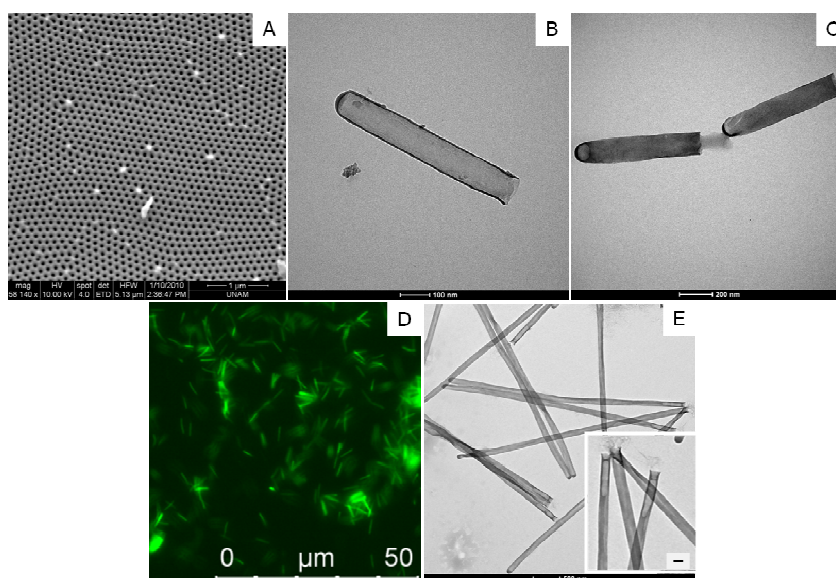


Fig. 2. (A) SEM of AAO membrane. (B) TEM of naked SNTs. (C) TEM of composite SNTs. (D) Fluorescence micrograph longer composite SNTs. Here, for improved image quality and visualization, $\sim 4 \mu\text{m}$ long composite SNTs filled with fluorescein-o-acrylate-containing gel (instead of DOX) were imaged. (E) TEM of the $\sim 4 \mu\text{m}$ long composite fluorescent SNTs indicates complete gel filling along the tube walls. The inset shows protrusion of a small gel region at the open ends of test tubes (scale bar = 100 nm).

nm length were used. In order to utilize the interior of SNTs for drug loading, SNTs were immersed in a prepolymer solution while they were still embedded within the AAO template. The constituents of this prepolymer solution were carefully selected to create a pH responsive gel which contained a photoinitiator, a crosslinker, HEMA, AEM, PEG-EEM and DOX (See Supplementary Info. for pH responsive drug release from this gel formulation). After UV exposure, gel-filled composite SNTs were obtained, liberated by template dissolution and further characterized by TEM (Fig. 2C) which confirms the complete gel filling along the tube walls.

Filled composite SNTs were further characterized by fluorescence microscopy where the gel matrix involved an fluorescein-o-acrylate component instead of DOX for improved image quality (Fig. 2D). Here, for the ease of visualization, deeper AAO templates were used to obtain $\sim 4 \mu\text{m}$ -long composite SNTs ($d=93\pm 4 \text{ nm}$, $l=3964\pm 144 \text{ nm}$). These SNTs displayed smooth fluorescence over the $4 \mu\text{m}$ particle length. The TEM images (Fig. 2E) of these long tubes also showed that, except a small region at their open ends, the structures are filled. The inset indicates minor gel protrusions originating from the open ends of the tubular nanoparticles.

The outer surfaces of these nanocarriers were modified with folate moieties for effective targeting against folate-receptor-overexpressing SK-BR3 breast cancer cells.²² This conjugation was confirmed by zeta potential, FTIR (Fig. 3), as well as XPS analysis (Fig. S1) where naked SNTs were used due to their ease of preparation. Folate conjugation was achieved by an initial aminosilane coating²¹ on the SNT surface which was followed by amide bond formation between the amine groups and EDC/NHS-activated FA.^{23, 24} Fig. 3A shows the zeta potential variation between naked, amine-modified (NH_2 -SNTs), and FA-modified SNTs (FA-NH_2 -SNTs). The negative zeta potential of the naked SNTs results from the deprotonation of the silanol groups on the surface at neutral pH. When coupled with the amine functional groups, the surface charge increases to positive values as expected, due to the large pK_a of the primary amine groups.⁹ After the folate conjugation, the surface charge returns back to the native negative charge as the

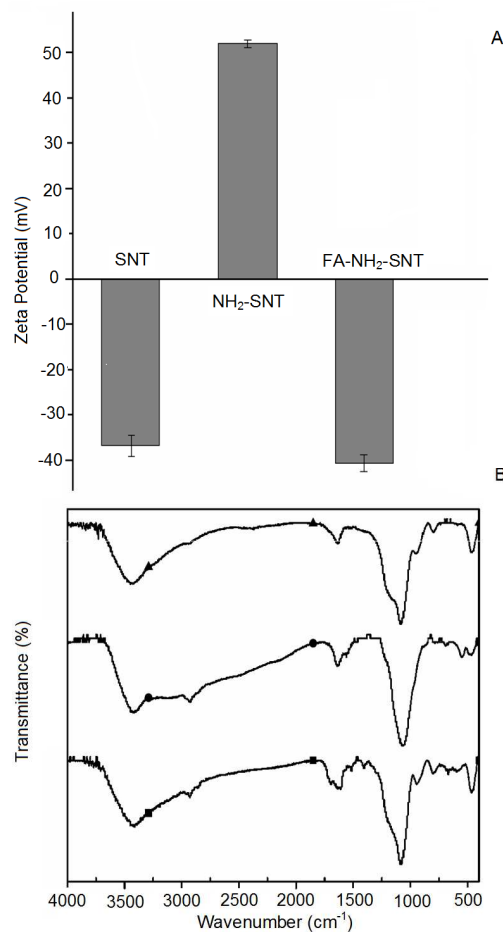


Fig. 3. The zeta potential (A) and FTIR measurements (B) for naked (\blacktriangle), amine (\bullet) and FA modified (\blacksquare) SNTs.

surface amine groups forms amide bonds and possible shielding of the surface by folate groups.²⁵ Fig. 3B presents the FT-IR spectra of SNTs, NH₂-SNTs, and FA-NH₂-SNTs. The band at 1083 cm⁻¹ in all the spectra was assigned to characteristic absorption band of Si-O. The appearance of the 1562 cm⁻¹ band results from the bending mode of NH- vibration for the NH₂-SNTs.²⁶ Finally, the FA-coupled tubes display the bands at 1514 and 1406 cm⁻¹, which were assigned to the absorption of the phenyl and pterin ring.²⁷

Fig. 4 depicts the cell viability data for SK-BR3 breast cancer cells and MCF-12A normal breast epithelial cells against SNTs with different compositions and concentrations. Here, SNTs 3,4 and 5 were composite structures with gel load but only the latter two contain the drug (Table 1). In all cases, average cell viabilities decreased with increasing particle concentration, and for both cell types significant cell death was observed only when the SNTs contain DOX (SNT4 and SNT5). The most notable result of Fig. 4 is the importance of targeting on inducing cell death as SNT5 is more cytotoxic than SNT4 for both cancer and normal cells. The two drug carriers differ only by the surface folate groups, and the influence of this group presents much more dramatic results for the cancer cells.

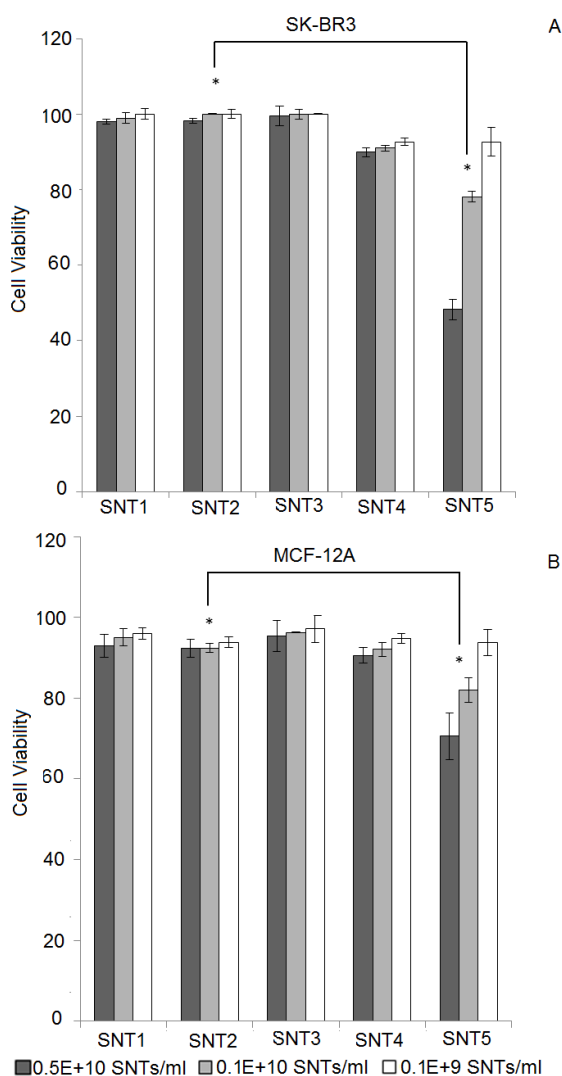


Fig. 4. Cell viability experiments of 48 h treated A) SK-BR3 and B) MCF-12A by using WST-1 Kit Assay (* $P < 0.05$).

The rationale behind this observation can be explained as follows: Although to a small extent, normal breast cells have folate receptors on their surface.²⁸ The presence of the folate targeting groups on drug-loaded SNTs causes increased particle cell interaction, nanocarrier internalization and hence cytotoxicity values for MCF-12A cells. The effect is more pronounced for cancer cells since the receptor is overexpressed on their membrane surface.²² Moreover, the nanocarrier is filled with a pH-responsive matrix that causes enhanced swelling and drug release within the acidic tumor milieu which further contributes to the cytotoxicity difference between normal and cancer cells.

Table 1. The composition of different SNT forms used in cell viability experiments.

Sample Code	SNT Content
SNT1	FA(-) Gel(-) DOX(-)
SNT2	FA(+) Gel(-) DOX(-)
SNT3	FA(+) Gel(+) DOX(-)
SNT4	FA(-) Gel(+) DOX(+)
SNT5	FA(+) Gel(+) DOX(+)

In order to compare their effectiveness, cell viability results of SNTs were compared with those of free DOX. Knowing the individual nanotube interior volume and used drug concentration for the gel, it can be deduced that ~ 50 ng/ml drug (or ~ 4500 DOX molecules / tube, see Supplementary Information for details) was used for SNT5 at 0.5×10^{10} particle concentration. This formulation induced 51.7 ± 2.7 % cell death, larger than the cytotoxicity value (46.0 ± 2.1 %) of the most concentrated free drug formulation in our studies (200 ng/ml, Figure S3). Hence, lower cell viabilities were obtained with much lower drug contents when SNTs were used as nanocarriers. Similar results were also reported by other effective nanocarrier systems^{17,22} and such nanostructures emerge as candidates for the treatment of drug-resistant cells or to reduce systemic toxicity problems

Conclusions

In conclusion, a novel route to prepare 1D silica-based multifunctional nanocomposites was introduced. Tubular structures were fabricated by using nanoporous AAO templates, and as demonstrated by the characterization studies, filled with a gel matrix to create composite nanostructures. The cell viability data revealed that, within the relatively high concentration regime employed, drug-lacking SNTs were effectively non-cytotoxic. More importantly, targeted SNTs with a drug payload can be successful candidates for cancer therapy as they showed increased cell killing for cancer cells when compared to control healthy cells and they induced larger cytotoxicity compared to free drug. This study is an initial effort which paves the way for targeted cancer therapy with such nanocomposites and we are currently investigating the cell internalization behaviour and in vivo cancer targeting opportunities of these deliberately engineered structures.

Acknowledgements

This work was supported by Marie Curie International Reintegration Grant within the 7th European Community Framework Programme (Grant No: 248819). We thank Dr. Gokhan Demirel from Gazi University for his generous support regarding the FA modification of SNTs and Hande Yegenoglu for the cell studies.

Notes and references

Electronic Supplementary Information (ESI) available: The details of AAO and SNT fabrication, SNT modification and characterization, cell culture experiments, free drug cytotoxicity, drug loading capacity and bulk gel release experiments are presented.

- 1 P. Couvreur, *Adv. Drug Deliv. Rev.*, 2013, **65**, 21.
- 2 M. Ferrari, *Nat. Rev. Cancer*, 2005, **5**, 161.
- 3 Y. Y. Wang, B. Li, L. M. Zhang, H. Song and L. G. Zhang, *ACS Appl. Mater. Inter.*, 2013, **5**, 11.
- 4 M. Talekar, J. Kendall, W. Denny and S. Garg, *Anti-Cancer Drugs*, 2011, **22**, 949.
- 5 J. H. Park, G. von Maltzahn, L. L. Zhang, M. P. Schwartz, E. Ruoslahti, S. N. Bhatia and M. J. Sailor, *Adv. Mater.*, 2008, **20**, 1630.
- 6 Y. Geng, P. Dalhaimer, S. S. Cai, R. Tsai, M. Tewari, T. Minko and D. E. Discher, *Nat. Nanotechnol.*, 2007, **2**, 249.
- 7 E. Heister, E. W. Brunner, G. R. Dieckmann, I. Jurewicz and A. B. Dalton, *ACS Appl. Mater. Inter.*, 2013, **5**, 1870.
- 8 H. Hillebrenner, F. Buyukserin, J. D. Stewart and C. R. Martin, *Nanomedicine*, 2006, **1**, 39.
- 9 H. Hillebrenner, F. Buyukserin, M. Kang, M. O. Mota, J. D. Stewart and C. R. Martin, *J. Am. Chem. Soc.*, 2006, **128**, 4236.
- 10 F. Buyukserin, C. D. Medley, M. O. Mota, K. Kececi, R. R. Rogers, W. H. Tan and C. R. Martin, *Nanomedicine*, 2008, **3**, 283.
- 11 B. He, S. J. Son and S. B. Lee, *Anal. Chem.*, 2007, **79**, 5257.
- 12 D. T. Mitchell, S. B. Lee, L. Trofin, N. Li, T. K. Nevanen, H. Soederlund and C. R. Martin, *J. Am. Chem. Soc.*, 2002, **124**, 11864.
- 13 X. Bai, S. J. Son, S. X. Zhang, W. Liu, E. K. Jordan, J. A. Frank, T. Venkatesan and S. B. Lee, *Nanomedicine*, 2008, **3**, 163.
- 14 C.-C. Chen, Y.-C. Liu, C.-H. Wu, C.-C. Yeh, M.-T. Su and Y.-C. Wu, *Adv. Mater.*, 2005, **17**, 404.
- 15 S. J. Son, J. Reichel, B. He, M. Schuchman and S. B. Lee, *J. Am. Chem. Soc.*, 2005, **127**, 7316.
- 16 C. R. Martin, *Science* 1994, **266**, 1961.
- 17 L. Wang, M. Kim, Q. Fang, J. Min, W. I. Jeon, S. Y. Lee, S. J. Son, S. W. Joo and S. B. Lee, *Chem. Commun.*, 2013, **49**, 3194.
- 18 H. Masuda and K. Fukuda, *Science*, 1995, **268**, 1466.
- 19 N. I. Kovtyukhova, T. E. Mallouk and T. S. Mayer, *Adv. Mater.*, 2003, **15**, 780.
- 20 F. Buyukserin and C. R. Martin, *Appl. Surf. Sci.*, 2010, **256**, 7700.
- 21 M. C. Kang, L. Trofin, M. O. Mota and C. R. Martin, *Anal. Chem.*, 2005, **77**, 6243.
- 22 J. Lu, M. Liong, Z. X. Li, J. I. Zink and F. Tamanoi, *Small*, 2010, **6**, 1794.
- 23 M. Wissink, R. Beernink, J. Pieper, A. Poot, G. Engbers, T. Beugeling, W. van Aken and J. Feijen, *Biomaterials*, 2001, **22**, 151.
- 24 H. Yang, Y. Zhuang, H. Hu, X. Du, C. Zhang, X. Shi, H. Wu and S. Yang, *Adv. Funct. Mater.*, 2010, **20**, 1733.
- 25 X. H. Wang, A. R. Morales, T. Urakami, L. F. Zhang, M. V. Bondar, M. Komatsu and K. D. Belfield, *Bioconjugate Chem.*, 2011, **22**, 1438.
- 26 S. McCarthy, G. Davies and Y. Gun'ko, *Nat. Protoc.*, 2012, **7**, 1677.
- 27 P. Huang, L. Bao, C. L. Zhang, J. Lin, T. Luo, D. P. Yang, M. He, Z. M. Li, G. Gao, B. Gao, S. Fu and D. X. Cui, *Biomaterials*, 2011, **32**, 9796.
- 28 M. S. Jhaveri, A. S. Rait, K.-N. Chung and e. al., *Mol. Cancer Ther.*, 2004, **3**, 1505.

